Physica C 470 (2010) 835–839

Contents lists available at ScienceDirect

Physica C

journal homepage: www.elsevier.com/locate/physc

Vortex motion in high-T_c films and a micropattern-induced phase transition

R. Wördenweber [a,*], E. Hollmann [a], J. Schubert [a], R. Kutzner [a], A.K. Ghosh [b]

[a] Institut für Bio- und Nanotechnologie (IBN) and JARA-Fundamentals of Future Information Technology, Forschungszentrum Jülich, D-52425 Jülich, Germany
[b] Department of Physics, Jadavpur University, Kolkata 700 032, India

ARTICLE INFO

Article history:
Available online 20 February 2010

Keywords:
Vortex matter
Vortex manipulation
Anomalous Hall effect
Guide motion of vortices
High-T_c films

ABSTRACT

A micropattern-induced transition in the mechanism of vortex motion and vortex mobility is observed in high-T_c thin films. The competition between the anomalous Hall effect and the guidance of vortices by rows of microholes (antidots) lead to a sudden change in the direction of vortex motion that is accompanied by a change in the critical current density and microwave losses. The latter effect demonstrates the difference in vortex mobility in different phases of vortex motion in between and within the rows of antidots.

1. Introduction

The dynamics of magnetic flux quanta (vortices) in superconductors shows similarity with that of quanta of electrical charge (electrons) in solids [1]. Exploring ways to control the motion of vortices has turned out to be useful for the understanding of vortex physics, for the improvement of existing superconducting devices, and for the development of innovative fluxtronic devices that employ vortices instead of electrons. Superconductors with periodic arrangements of pinning centres are suitable systems for studying dynamic phenomena of vortex movement. Beginning with the demonstration of commensurability effects in superconducting thin films with regular arrays of sub-micrometer holes (antidots) serving as artificial defects [2–6], we could demonstrate that local vortex trapping and guidance of magnetic flux motion can be achieved via strategically positioned antidots and antidot arrays [7,8]. Appropriate periodic antidot structures breaking the symmetry of the vortex pinning potential [8–11] resulted also in vortex ratchet effect, observed in both low- and high-T_c thin films [12]. This effect suggests the feasibility of more complex fluxtronic device concepts. In all these concepts, the manipulation of vortices via patterning will be essential.

The purpose of our work presented here was to investigate the possibility of inducing a transition from unguided to guided vortex motion within suitably patterned high-T_c thin films. We demonstrated that a properly designed arrangement of arrays of antidots in high-T_c films can lead to guided vortex motion that sets in at a clearly defined temperature. The transition from unguided to guided vortex motion and the resulting change in the mobility of vortices were demonstrated via combined dc and microwave measurements.

2. Sample preparation and experimental techniques

We deposited high-T_c films of $YBa_2Cu_3O_{7-\delta}$ (YBCO) via pulsed laser deposition or magnetron cathode sputtering on microwave-compatible substrates of either $LaAlO_3$ or CeO_2-buffered sapphire. The CeO_2 buffer layers had a thickness of ~30 nm. For YBCO we chose a film thickness of $d \approx 50$–100 nm to obtain a large effective penetration length and low critical currents. The latter property is important to avoid local heating, especially at contact pads during flux flow experiments. The zero-temperature effective penetration depth $\lambda_{eff} = \lambda_L \coth(d/2\lambda_L)$ [13] is about ~1.4 μm to ~0.7 μm in our 50–100 nm thick YBCO films. The lattice mismatch between YBCO and the substrate (2% for $LaAlO_3$ and 10–12% for r-cut sapphire) resulted in a slight reduction of the transition temperature. T_c values range from 88 to 89 K for YBCO on sapphire.

To guide vortices, arrays of small holes (antidots) were patterned in our films via optical lithography and ion beam etching. In experiments discussed here, pairs of parallel rows of antidots having the nominal diameter of 1.2 ± 0.05 μm have been used. The spacing of antidot centers in each row pair was 6 μm, the distance of adjacent antidot centers between neighboring row pairs was ~12 μm, as shown in the microscopic image of Fig. 1. Inset in that figure shows schematically the sample design. The film strip along x axis can serve as a stripline for microwave signals. In superconducting state, when dc current I is applied along the x axis of the sample (at ports 1 and 2), and $d \ll \lambda_{eff}$, the Lorentz force F_L perpendicular to I acts on the vortices along the y axis. With decreasing temperature T, $F_L(I)$ increases and simultaneously the strength of vortex–antidot interaction increases too. Below a certain

* Corresponding author. Tel.: +49 2461 61 2365; fax: +49 2461 61 2470.
E-mail address: r.woerdenweber@fz-juelich.de (R. Wördenweber).

0921-4534/$ - see front matter © 2010 Elsevier B.V. All rights reserved.
doi:10.1016/j.physc.2010.02.083

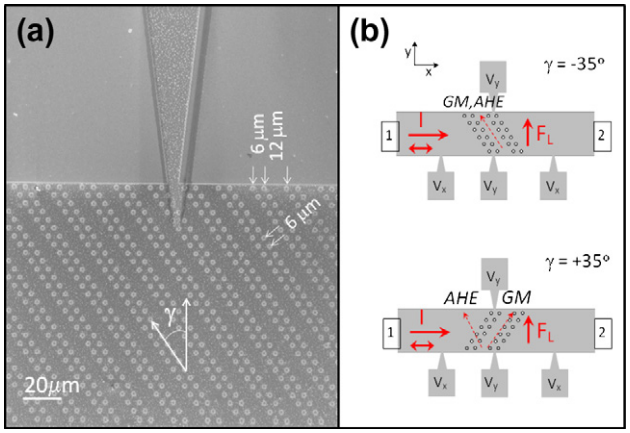

Fig. 1. (a) Microscopic image of a section of a sample depicting one of the Hall contacts and the configuration of antidot rows. (b) Schematics of sample design with two different orientations of rows: $\gamma = -35°$ and $\gamma = +35°$. The angle γ is defined by the nominal direction of the Lorentz force and the orientation of rows. The voltage probes, input and output ports for dc and rf current (1, 2), the directions of current, Lorentz force, anomalous Hall effect (AHE) and guided motion (GM) are shown.

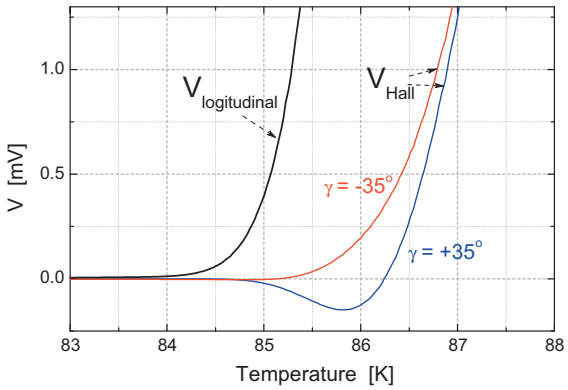

Fig. 2. Temperature dependence of the longitudinal voltage (contacts V_x) and Hall signals (contacts V_y) at the transition temperature. Depending on the direction of rows of antidots contacts the anomalous Hall effect is present ($\gamma = +35°$) or suppressed ($\gamma = -35°$).

temperature they will move along each row. We chose the angle γ between the row direction and the y axis to optimize the Hall signal voltage V_y due to guided motion of vortices. According to the simplified "1-channel model" [8], in which the flux is expected to drift predominantly along the row of antidots, the component of the Lorentz force, which compels vortices to move along the antidot rows (*i.e.* guided motion), is $F_{guid} = F_L \cos\gamma$. Here F_L is the modulus of the Lorentz force $F_L = |F_L|$. In turn, it is the component of the Lorentz force parallel to the applied current $F||_{guid} = F_{guid} \sin\gamma = F_L \cos\gamma \sin\gamma$, that contributes to the Hall voltage and finally leads to the Hall signal which is given by $V_{Hall} \propto F_L \cos\gamma \sin\gamma$. The experimentally determined angular dependence of V_{Hall} roughly obeys this simple relation. Specifically, the maximum Hall voltage is obtained for $\gamma = 30–40°$ [14,15] while the 1-channel model predicts a maximum at 45° [8]. We thus fabricated and characterized two sample types, one with $\gamma = +35°$, and another with $\gamma = -35°$.

We analyzed critical dc properties of our films and the vortex dynamics in the superconducting state, between approximately $T = 82$ K and T_c, via combined resistive and microwave 6-probe measurements. A microwave signal in the frequency range between 0.05 and 20 GHz, with up to 5 dBm maximum input power, was superposed on the dc current applied to the superconducting stripline. The current (dc and microwave) was inserted at ports 1 and 2 (see Fig. 1). The microstrip and the ports were 50 Ω impedance-matched. The voltage contacts were small in size and designed to minimize microwave penetration into the dc measurement setup. The longitudinal and transverse (*i.e.*, Hall signal) components of the dc voltage, V_x and V_y, characterized the transverse ($\langle v_y \rangle$) and longitudinal ($\langle v_x \rangle$) components of vortex motion velocity, respectively. The microwave transmission coefficient S_{21} was simultaneously recorded to provide a measure for losses resulting from vortex motion. The dc voltages were measured by Keithley nanovoltmeter 181. The Hewlett Packard network analyzer HP8720D was used to measure S_{21}. Low-intensity dc magnetic fields were applied normal to the film surface using normal Helmholtz coils to generate vortices. Field range up to a few millitesla was chosen to avoid inducing interstitial vortices between the antidots.

3. Experimental results and discussion

Definitions of measured parameters: The longitudinal voltage represents the standard parameter to characterize the critical properties of a superconducting stripline. In the normal regime, $V_{longitudinal}$ represents the normal state resistivity, whereas in superconducting regime, it is generated by vortex motion along the Lorentz force, *i.e.*, across the stripline. In the latter case, $V_{longitudinal}$ characterizes the average velocity component $\langle v_y \rangle$ of vortex, *i.e.*, is a measure for the flux transfer across the stripline collected between the longitudinal voltage contacts labeled V_x in Fig. 1.

The Hall signal in superconducting regime characterizes the vortex motion along the stripline. The chosen arrangement of Hall contacts (labeled V_y in Fig. 1) makes possible the analysis of the component of vortex motion parallel or antiparallel to the current. Furthermore, it enables a more local analysis of the vortex motion that is restricted to the vicinity of the contacts pair. High-T_c materials typically reveal the, so-called, anomalous Hall effect (AHE), *i.e.*, the sign inversion of the Hall signal below T_c [14,16–24]. It has been shown, that the AHE in high-T_c material is caused by vortex motion. Most likely the additional component of vortex motion is caused by the Magnus force acting on the very weakly pinned vortices, close to T_c [14]. Depending on the orientation of the rows of antidots, the AHE can be suppressed or not. This is demonstrated in Fig. 2. It shows the transition to the superconducting state determined by the measurements of the longitudinal voltage together with the temperature dependence of the Hall signals for both designs $\gamma = +35°$ and $\gamma = -35°$. Whereas the Hall contacts positioned at antidots rows with $\gamma = +35°$ display the AHE, the Hall signal measured at antidots rows with orientation $\gamma = -35°$ do not show signs of an AHE.[1]

Additionally to the transition temperature, the critical current density J_c can be recorded via the different contacts. The standard J_c value is defined by measurements of the longitudinal voltage (voltage contacts V_x). The longitudinal voltage is kept constant (typically at a value of a voltage criterion of a few µV/cm) and the resulting current defines the critical current $I_c = J_c\, dw$ (d and w represent the thickness and width of the stripline). For our samples, $J_c(T)$ shows the classical behavior for both arrangements of rows of antidotes (with positive and negative angle γ). Except for temperatures near the transition from normal state, J_c increases linearly with decreasing temperature.

Similar to measurements of the classical critical current, we could keep the component of vortex motion $\langle v_x \rangle$ constant by con-

[1] Please note, that the longitudinal voltage collects the total flux transport across the stripline registered between the voltage contacts V_x whereas the Hall signal records the vortex motion 'across the imaginary line between each pair of Hall contacts V_y'. Consequently, the longitudinal voltage signal is orders of magnitudes larger compared to the Hall signal for the case of vortex motion. Therefore a finite signal $V_{longitudinal}$ persists to lower temperatures where the Hall signal is already so small that it cannot be measured.